Electronic Supplementary Material (ESI) for Physical Chemistry Chemical Physics

Supplementary Information for

Effect of Interface on Surface Morphology and Proton Conduction of Polymer Electrolyte Thin Films

Akihiro Ohira*[a,b], Seiichi. Kuroda*[b], Hamdy F. M. Mohamed[b,c], and Bruno Tavernier[b]

[a] Research Institute for Ubiquitous Energy Devices, National Institute of Advanced Industrial Science and Technology (AIST), 1-8-31, Midorigaoka, Ikeda, Osaka 563-8577, Japan

[b] Fuel Cell Cutting-Edge Research Center (FC-Cubic), Technology Research Association, 2-3-26 Aomi, Koto-ku, Tokyo 135-0064, Japan

[c] Present address: Physics Department, Faculty of Science, Minia University, P.O. Box 61519 Minia, Egypt.

Contents:

Comparison of surface roughness of thin films on different substrates determined by AFM images (1 x 1 μm^2). Relationship between SCD values and proton conductivity for NR212 membrane.

Figure S1. Schematic illustration demonstrating the principle of atomic force microscopy coupled with an electrochemical (e-AFM) imaging technique.

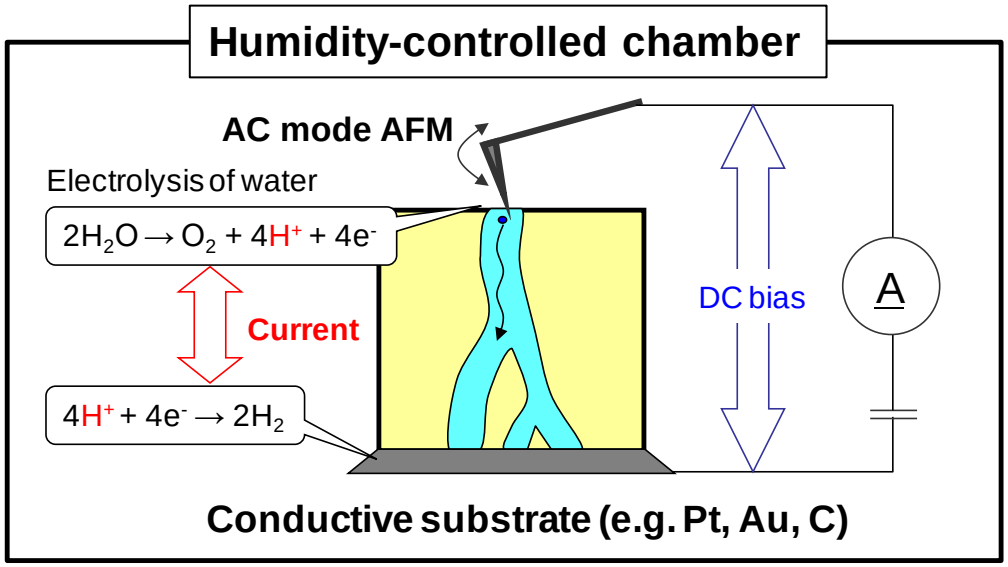

A schematic drawing of the instrument for atomic force microscopy coupled with an electrochemical (e-AFM) system is shown in Figure S1. A humidifier unit was used to control the internal humidity of the AFM chamber. Samples, consisting of a thin film on a substrate, were placed on the gold-plated conductive stage fixed with conductive paste such as colloidal graphite. During characterization, a bias voltage was applied between the tip and sample stage. If current was detected, it was taken as an indication that the tip had come in contact with water present on an active proton path. When the tip contacted the water, protons were generated

through electrolysis. They were transported to the opposite side through the thin film and reacted with electrons to form hydrogen at the interface of thin film and sample stage. If the tip contacted water in an inactive region (disconnected from the bottom), no current was detected. Therefore, the mapping of these currents generated images of proton-conducting regions.

Table S1. Comparison of film thicknesses determined by ellipsometry, Doppler broadening of annihilation radiation (DBAR), and atomic force microscopy (AFM) scratch analyses. (GC, glassy carbon)

Sample	**Ionomer concentration (%)**	**Ellipsometry (nm)**	**DBAR (nm)**	**AFM (nm)**
GC	0.10	–	–	5.8
GC	0.25	~9-11	~7	11.5
GC	0.50	~15	~14	17.4
Pt/GC	0.10	–	~5	5.1
Pt/GC	0.25	~7	~8	11.2
Pt/GC	0.50	~21	~24	19.6
Pt/GC	1.00	~37	~40	40.2

The thickness of the films was determined by various destructive methods. First, spectroscopic ellipsometry (FE5000S, Otsuka Electronics) was performed to determine the ionomer film thickness using the isotropic *n*-Cauchy model. The values obtained were then cross-checked with positron annihilation spectroscopy (PAS); Doppler broadening of annihilation radiation (DBAR)

spectra were measured as a function of positron incident energy (0-30 keV) using a slow positron beam.[1] Energetic positrons emitted from a sealed ^{22}Na positron source with an activity of 1.11 GBq (from Amersham) were moderated using a tungsten mesh. The 0.511 MeV annihilation γ-rays were measured with a high resolution γ-ray spectrometer. Each DBAR spectrum was characterized by the S parameter, which was defined as the ratio of the central area (510.3–511.7 keV) to the total counts of the annihilation peak. The total counts for each DBAR spectrum was 1.2 million after subtracting the background. The relationship between the S parameter and positron energy was determined using the VEPFIT program[2] to estimate the thickness of the ionomer film. Details of the fitting model and its procedure are described elsewhere.[3,4]

Y. Kobayashi, I. Kojima, S. Hishita, T. Suzuki, E. Asari and M. Kitajima, *Phys. Rev. B,* 1995, **52**, 823–828.

A. van Veen, H. Schut, J. de Vries, R. A. Hakvoort and M. R. Ijpma, *AIP Conf. Proc.,* 1990, **218**, 171–196.

A. van Veen, H. Schut, M. Clement, J. M. M. de Nijs, A. Kruseman and M. R. IJpma, *App. Surf. Sci.,* 1995, **85**, 216–224.

H. Schut and A. van Veen, *J. Phys. IV France,* 1995, **05 C1**, C1-57–C1-61.

Figure S2. Image of water contact angle on glassy carbon (GC) and Pt/GC surfaces before and after UV-ozone treatment.

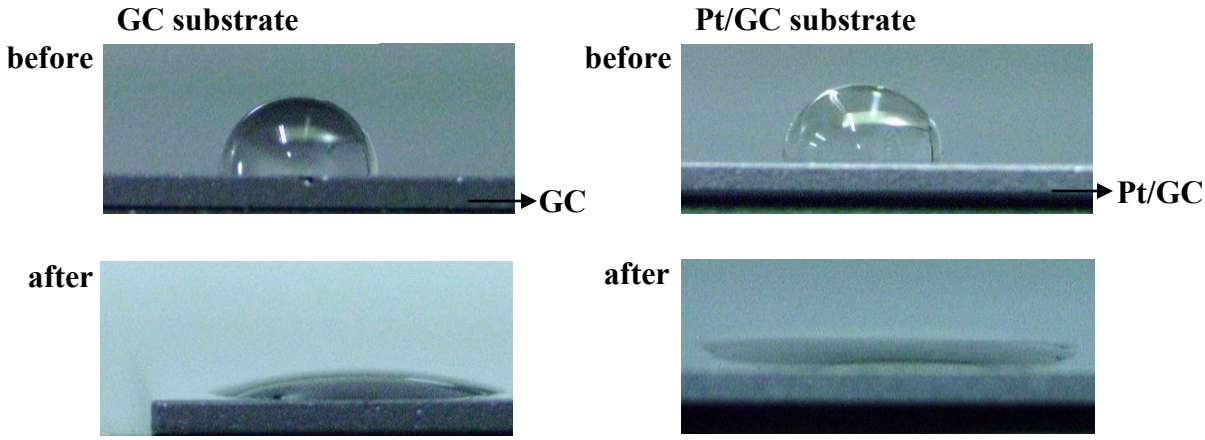

Here, we used UV-ozone treatment to change the surface hydrophilicity of the GC substrate. Unfortunately, we could not detect a significant difference using attenuated total reflectance infrared (ATR-IR) spectroscopy because of the very low refracted signal intensity from the carbon surface because water spread on substrate after treatment, as the surface turned out to be the hydrophilic-GC substrate. For Pt/GC substrates, the main purpose was to remove organic contaminants from the surface just after sputtering. Therefore, we used untreated GC substrates, treated GC substrates (hydrophilic-GC), and treated Pt/GC substrates for this study.

Figure S3. Typical AFM current-mapping and phase images of ionomer thin (12.4 nm, A and B) and thick films (221 nm, E and F) on glassy carbon (GC) substrates. The images (A and E) and (B and F) correspond to current-mapping and phase images, respectively. Each current-mapping and phase image was binarized as shown in black and white picture at lower part of each image.

The focus was put on their high current density and soft phase domains (black color) in each image. Scan size: 200 × 200 nm^2. Conditions: 22°C, 85 %RH. In these images, blue circle shows the point where proton conductive and hydrophilic region are well-matched each other at the same place while the area into red circle indicates the part of nonconformity between proton conductive and hydrophilic region.

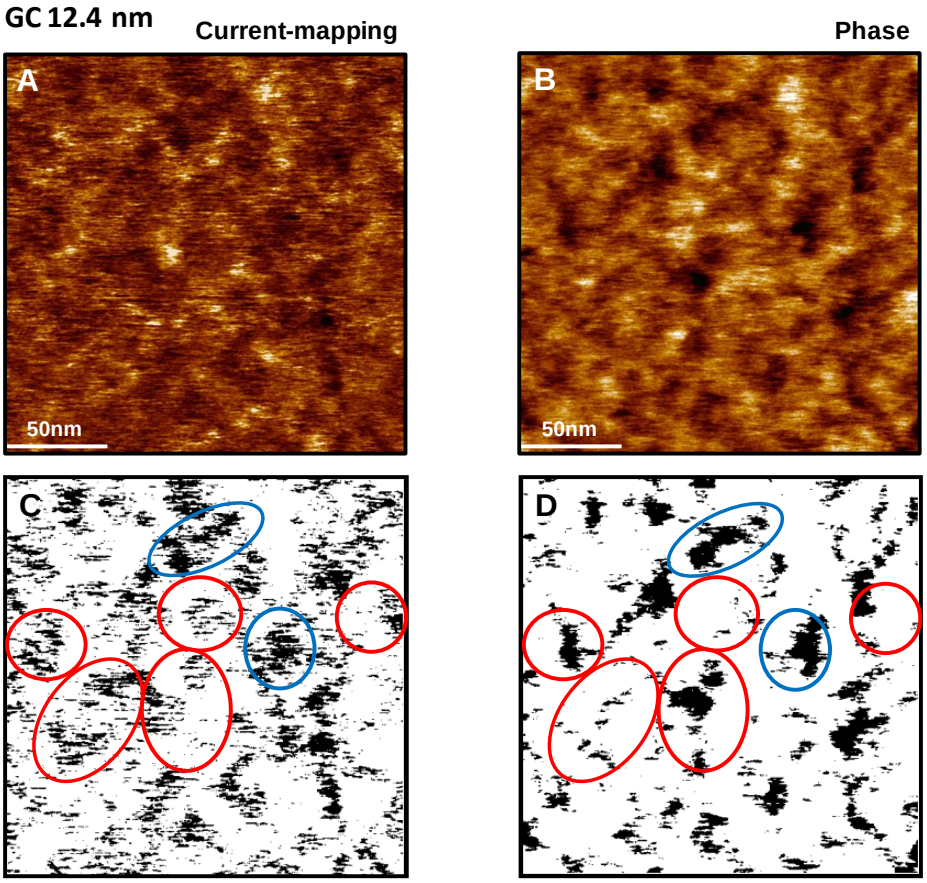

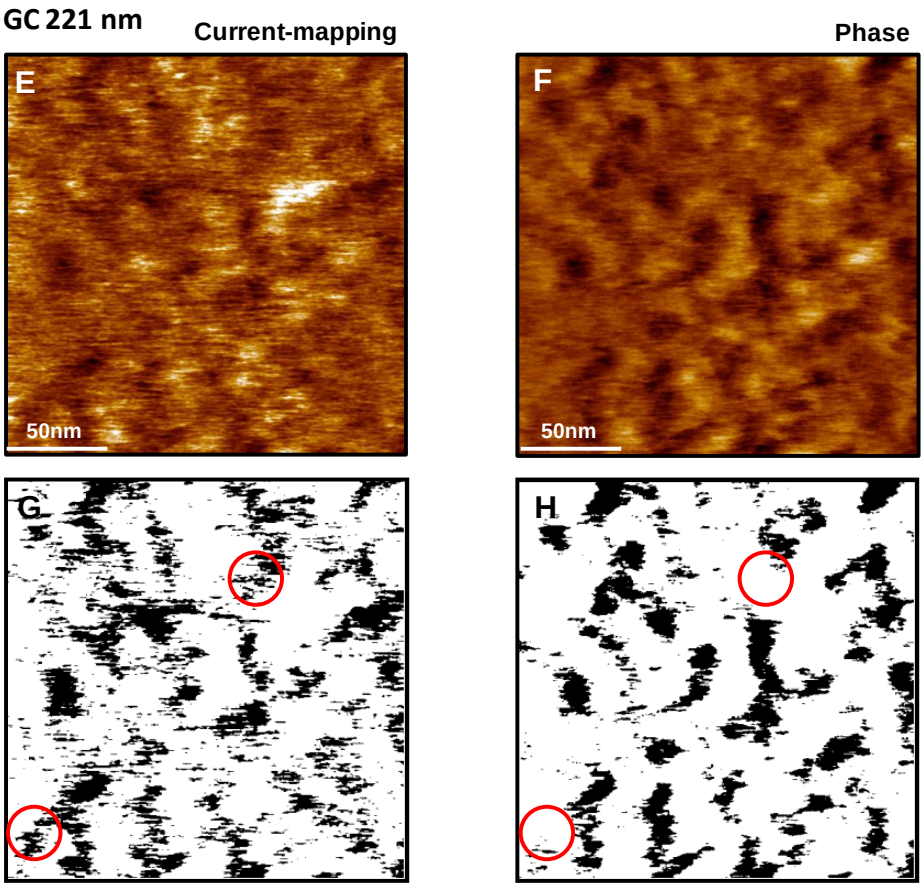

For thinner film, it can be clearly seen that the area into red circle is noticeable compared to the blue one. This indicates that hydrophilic domains in the film are not necessarily integrated into the "active proton path," which connects the top and bottom of the film and also points out disordered surface morphology. On the contrary, for thicker film, although some nonconformity parts can be seen in red circle between current-mapping and phase images most of region seems to be good agreement with proton conductive and hydrophilic domains. Furthermore each conductive domain for thicker film is gathered and is larger than that for thinner film. This difference also implies that phase separation between hydrophobic and hydrophilic domains is well-developed in thicker films than in thinner one.

Figure S4. Atomic force microscopy (AFM) (A and C) topographic and (B and D) phase images of ionomer thin films prepared from 0.1% Nafion® dilute solution on glassy carbon (GC) substrates scanned using high and low spring constant cantilevers under humidified conditions (22 °C, 85% relative humidity (RH)).

A and B: Scanned using a low spring constant cantilever (3.0 N/m, 75 KHz), thickness: 5.8 nm

C and D: Scanned using a high spring constant cantilever (40 N/m, 300 KHz), thickness: 5.9 nm

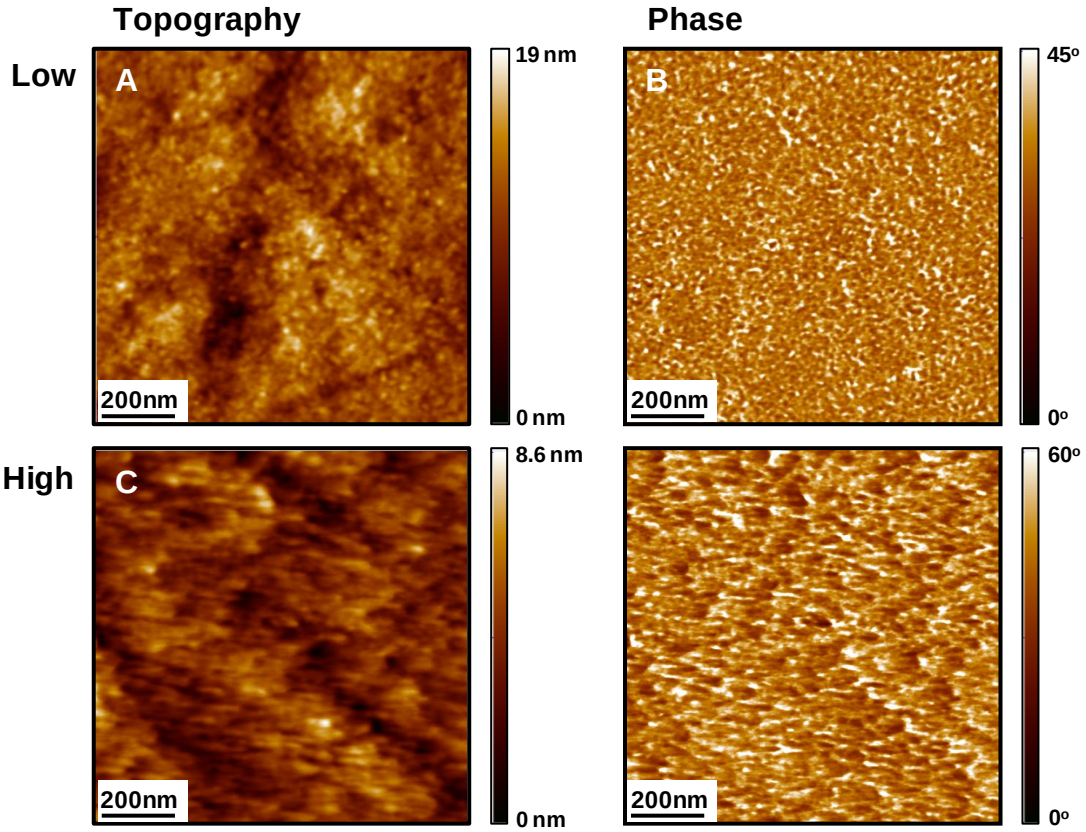

In comparing images of A and C, large and indistinct boundaries can be seen in C. Furthermore, these boundaries are somewhat dragged in the lateral direction (scan direction). A similar trend can be seen in phase image D. This dragged property could not be improved even by reducing

the contact force between the tip and interface. On the other hand, in images A and B scanned using a low spring constant cantilever, a small particle is obviously seen in A and the corresponding phase separated morphology is recognizable in B. The low spring constant cantilever produces high reproducibility imaging even under high RH conditions. This indicates that appropriate experimental conditions are required for AFM imaging for thin films in particular, and that cantilevers with a high spring constant cannot be used for acquiring images of thin films on substrate in this study.

Figure S5. Relationship between the surface current density (SCD) value and proton conductivity for NR212 membrane.

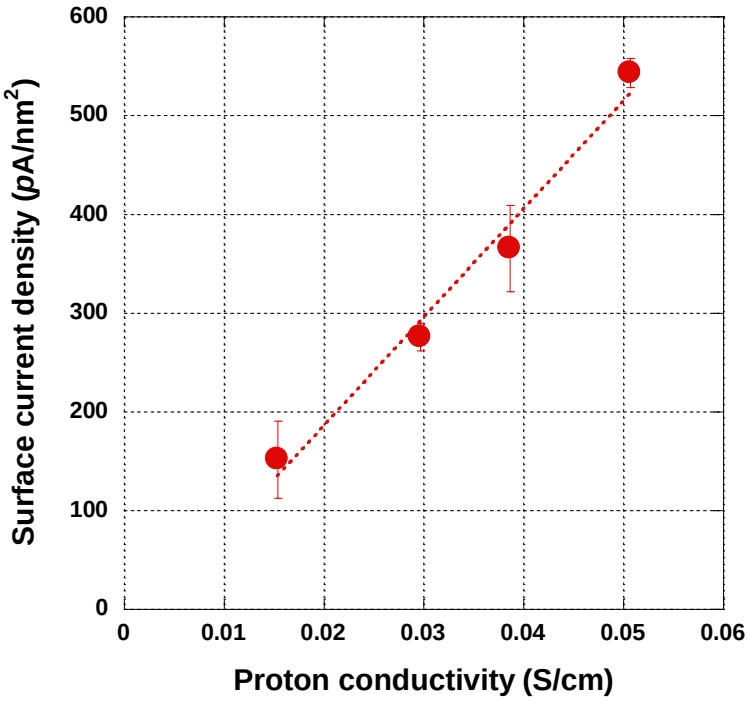

Surface current density (SCD) values were estimated by integrating the current-distribution profiles taken from 1 × 1 □m^2 regions of current-mapping images. The SCD value is defined as follows:

$$\mathbf{SCD} = \frac{\sum_{i=1}^{k} N_i I_i}{A}$$

Here, N_i is number which indicates the quantity of pixels that possess a current value I_i in the image (512 x 512 pixels), A is the scanned area of 1000 x 1000 nm^2 and k is the total amount of the bins in the histogram (in our case 256 bins). Proton conductivity was measured using a four-point probe method. Proton conductivity at 25 °C under partially hydrated conditions was measured using a home-made window cell geometry and a Ivium Stat (Ivium Technologies B.V. The Netherlands) over a frequency range from 1 Hz to 100 kHz. Since there was no large deviation in whole frequency ranges, the real part of the impedance value at 1 kHz was used for the estimation of conductivity. Membranes were equilibrated in a humidity–temperature oven (Espec, SH-241) at the specified relative humidity (RH) for at least 60 min before characterization. The proton conductivity of each sample was calculated from dry membrane thickness and membrane resistance taken at the frequency that produced the minimum imaginary response.

In Figure S5, a good linear correlation between SCD and proton conductivity was observed at all relative humidity conditions tested. This result clearly indicates that SCD is related to proton

conductivity and can be used as a proxy measurement for proton conductivity. In this study, we adopted the SCD value at higher relative humidity (~85% RH) for comparison.

Table S2. Comparison of surface roughness of thin films on different substrates determined by AFM image (1 x 1 μm^2).

Topographic images (1000 x 1000 nm)	Roughness average (Ra) (nm)	Maximum height (Rz) (nm)	Film thickness (nm)
Film on GC	1.44	17.70	5.8
Film on hydrophilic-GC	1.70	16.57	5.9
Film on GC/Pt	1.85	14.89	5.1
GC (bare)	1.88	16.64	-

The value of surface roughness calculated *via* roughness average (Ra) and maximum height (Rz) of topographic images (determined at 1 x 1 μm^2 scanned area) are equivalent for these three samples. Although Rz is higher than the film thickness the Ra and Rz of bare GC are quite similar to those of thin films, indicating that the roughness is contributed from the substrate but not from the film itself. There are abrasion traces onto the surface of GC due to mirror polishing. This characteristic mainly contributes to surface roughness. In our study, to avoid the negative effect by intrinsic characteristic as much as possible, we adopted 1 x 1 μm^2 scanned area to estimate SCD value because abrasion traces are not so much and resolution for determination of SCD value is suitable in this observation area. Therefore, we can compare the SCD value among thin films on different substrates.